

## Structural and chemical changes in binary versus ternary tetrahedral semiconductors

José Luís Martins and Alex Zunger  
Solar Energy Research Institute, Golden, Colorado 80401  
(Received 13 May 1985)

The properties of a prototype ternary semiconductor with the chalcopyrite structure—MgSiP<sub>2</sub>—are studied as a function of lattice constant, tetragonal distortion, and anion displacement with the use of the *ab initio* density-functional method. This system is then used as a general model for understanding the chemical and structural differences between a binary tetrahedral semiconductor (e.g., zinc blende) and its isoelectronic ternary analog (e.g., MgSiP<sub>2</sub>).

Fourfold-coordinated tetrahedrally bonded ternary  $A^{II}B^{IV}C_2^V$  semiconductors (e.g., MgSiP<sub>2</sub>, space group  $D_{2d}^{12}$ , Fig. 1) are related generically to their binary zinc-blende  $A^{III}C^V$  analogs (e.g., AlP, space group  $T_d^2$ ) in the same way as the latter are related to the diamondlike  $B^{IV}B^{IV}$  homopolar semiconductors (e.g., Si, space group  $O_h^7$ ). Much as a (hypothetical) nuclear disproportionation converts the diamond structure of <sup>14</sup>Si<sup>14</sup>Si into the zinc-blende structure <sup>13</sup>Al<sup>15</sup>P, so does an analogous cation disproportionation convert the (doubled unit cell) zinc-blende structure of <sup>13</sup>Al<sup>13</sup>AlP<sub>2</sub> into the chalcopyrite structure <sup>12</sup>Mg<sup>14</sup>SiP<sub>2</sub>. All three structure types show a fourfold tetrahedral coordination with an average of four electrons per atom (Grimm-Sommerfeld compounds) and exhibit covalent semiconducting properties.<sup>1</sup> However, whereas the diamond-to-zinc-blende sequence offers but a single added (chemical) feature (the distinction between a cation and an anion), the zinc-blende-to-chalcopyrite sequence offers, in addition to a new *chemical* degree of freedom (the distinction between one and two cations), two new *structural* degrees of freedom. These are<sup>2</sup> (i) the ability of the crystallographic *c* axis to deviate from twice the *a* axis (denoted here as the tetragonal distortion  $\eta \equiv c/2a$ ), and (ii) the ability of the anion to be displaced from its ideal tetrahedral site, creating two dissimilar anion-cation bond lengths  $R_{AC}$  and  $R_{BC}$  [a distortion denoted here by the bond-alternation parameter  $u \equiv \frac{1}{4}$

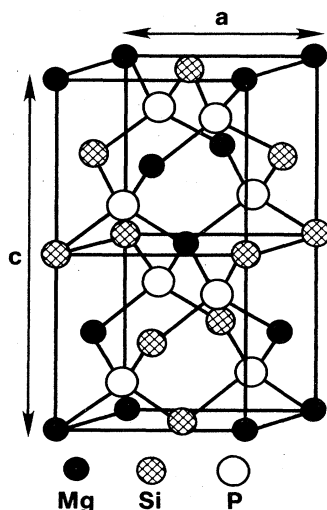


FIG. 1. Crystal structure of MgSiP<sub>2</sub>. The coordinates of the P atom on the lower left corner are  $(ua, a/4, c/8)$ .

+  $(R_{AC}^2 - R_{BC}^2)/a^2$ ]. In the diamond and zinc-blende structures  $\eta \equiv 1$ ,  $u \equiv \frac{1}{4}$ . The structural and chemical changes attendant upon the formation of a ternary *sp*-bonded tetrahedral structure from two binary systems are pertinent to the understanding of locally<sup>3</sup> or coherently<sup>4</sup> ordered solid solutions formed from binary semiconductors (e.g., GaAs + AlAs  $\rightarrow$  GaAlAs<sub>2</sub>). The simplistic but common<sup>5</sup> description of a ternary system, e.g., ABC<sub>2</sub>, in terms of a "virtual-crystal" approximation (VCA) ignores the added chemical and structural degrees of freedom by replacing ABC<sub>2</sub> with "average atoms," i.e.,  $\langle AB \rangle \langle AB \rangle C_2$  [or, in general, replacing  $A_x B_{1-x} C$  with  $\bar{A}C$ , where  $\bar{A} \equiv xA + (1-x)B$ ]. In so doing, the real differences in band structure, charge distribution, and total energy between the binary and ternary systems are obscured. Free from the complications of chemically active cation *d* orbitals which exist in other chalcopyrite compounds (e.g.,<sup>2</sup> ZnSiP<sub>2</sub>, CuInSe<sub>2</sub>), MgSiP<sub>2</sub> offers a natural example for studying the consequences of added chemical and structural degrees of freedom on the electronic properties of the system. In this paper we apply the pseudopotential total-energy minimization method<sup>6</sup> for the first time to a real ternary system—MgSiP<sub>2</sub>—and study the effect of the added chemical degree of freedom (by comparison with AlP in the same structure) as well as the structural degrees of freedom [by studying the surface  $F(a, \eta, u)$  for  $F$  set equal to the charge density, total energy, and band gaps] on its properties. This establishes the nature of the changes attendant upon formation of a ternary semiconductor from binary systems.

The electronic structure and total energy of MgSiP<sub>2</sub> are calculated in the Ihm, Zunger, and Cohen<sup>6</sup> self-consistent local-density pseudopotential formalism with a plane-wave basis set. We use the Ceperley-Alder exchange-correlation functional as parametrized by Perdew and Zunger<sup>7</sup> and the nonlocal pseudopotential of Bachelet, Hamann, and Schlüter.<sup>8</sup> The wave-function basis set includes all the plane waves with kinetic energy smaller than 12 Ry, which corresponds to using 700–800 plane waves. Special techniques were used to diagonalize the large Hamiltonian matrices,<sup>9</sup> and to accelerate convergence towards self-consistency.<sup>10</sup> In the final self-consistency iteration, components of the total potential change by less than 0.2 mRy. Integrations over the Brillouin zone were performed using the single special *k* point obtained from the two usual *k* points of the zinc-blende Brillouin zone by folding it into the chalcopyrite Brillouin zone.<sup>10</sup> The equilibrium structure was obtained by fitting a quadratic function of *a*,  $\eta$ , and *u* to the total energies  $E(a, \eta, u)$  calculated for 25 different geometries.

## BULK PROPERTIES

The calculated structural constants of  $\text{MgSiP}_2$  (Table I) agree to within 1%–3% with the experimental values,<sup>11</sup> showing that the pseudopotential local-density theory is able to predict not only the volume of the unit cell (as has been done before for binary semiconductors<sup>12</sup>), but also more subtle properties such as the tetragonal distortion and internal displacements. We have also included in Table I the predictions of the “conservation of tetrahedral bonds” (CTB) model, shown previously<sup>2</sup> to reproduce the trends in the structural parameters of chalcopyrite semiconductors. The present *ab initio* model is seen to be more accurate.

The analysis of the total-energy surface shows that  $\text{MgSiP}_2$  is very soft with respect to volume conserving (i.e.,  $a^2c = \text{const}$ ) distortions which alter the value of the tetragonal parameter  $\eta \equiv c/2a$ . The calculated values of the elastic moduli ( $\lambda_{xxxx} + \lambda_{xyxy}$ ,  $\lambda_{zzzz}$ , and  $\lambda_{xxzz}$  (in the notation of Landau and Lifshitz<sup>13</sup>) are 219, 69, and  $73 \times 10^9$  N/m<sup>2</sup>, respectively. These have not yet been measured (compare, however, with the similar values<sup>14</sup> of 230, 166, and  $64 \times 10^9$  N/m<sup>2</sup>, respectively, measured for Si). The calculated phonon frequency  $\omega_u$  of the chalcopyrite  $\Gamma_1$  optical phonon (derived from a zinc-blende  $W_1$  phonon) is  $320 \text{ cm}^{-1}$ . Although it has not been measured for  $\text{MgSiP}_2$ , it has been measured for several similar diphosphide compounds,<sup>15</sup> giving values in the range of  $310\text{--}330 \text{ cm}^{-1}$ . Since the  $\Gamma_1$  phonon involves only displacements of P atoms (associated with changes in  $u$ ), we expect the actual  $\Gamma_1$  phonon frequency of  $\text{MgSiP}_2$  to be in the same range, as predicted by our calculation.

## BAND STRUCTURE

The calculated band structure (Fig. 2) is similar to the one previously calculated for the experimental geometry with the all-electron, potential-variation mixed-basis (PVMB) method,<sup>2</sup> but deviates in some details from the results of previous empirical pseudopotential calculations.<sup>16</sup> There are three valence bands: (i) a phosphorus  $s$  band with some silicon  $s$  contribution, (ii) a Si-P band, and (iii) a predominantly phosphorus  $p$  band. The total valence-band width of 12.4 eV compares well with the experimental value<sup>17</sup> of  $12.8 \pm 0.9$  eV, and its main features agree with the observed x-ray photoemission spectra.<sup>17</sup> The top of the valence band has  $\Gamma_{4v}$  symmetry with a  $\Gamma_{5v}$  state lower in energy by the crystal-field (CF) energy  $\Delta_{CF} = \epsilon_{\Gamma_{4v}} - \epsilon_{\Gamma_{5v}}$ . Both

TABLE I. Comparison of calculated (calc) and experimental (Ref. 11) (expt) structural properties of  $\text{MgSiP}_2$  with those of its analogs AIP and Si. The predictions of the empirical CTB model (Ref. 2) are also shown.

	$a$ (Å)	$c/a$	$u$
$\text{MgSiP}_2$ (calc)	5.70	1.72	0.288
$\text{MgSiP}_2$ (expt)	5.718 <sup>a</sup>	1.769 <sup>a</sup>	0.292 <sup>a</sup>
$\text{MgSiP}_2$ (CTB)	5.63	1.87	0.284
AIP (calc)	5.41	...	...
AIP (expt)	5.467 <sup>b</sup>	...	...
Si (calc)	5.40	...	...
Si (expt)	5.431 <sup>c</sup>	...	...

<sup>a</sup>Reference 11.

<sup>b</sup>Reference 25.

<sup>c</sup>Reference 26.

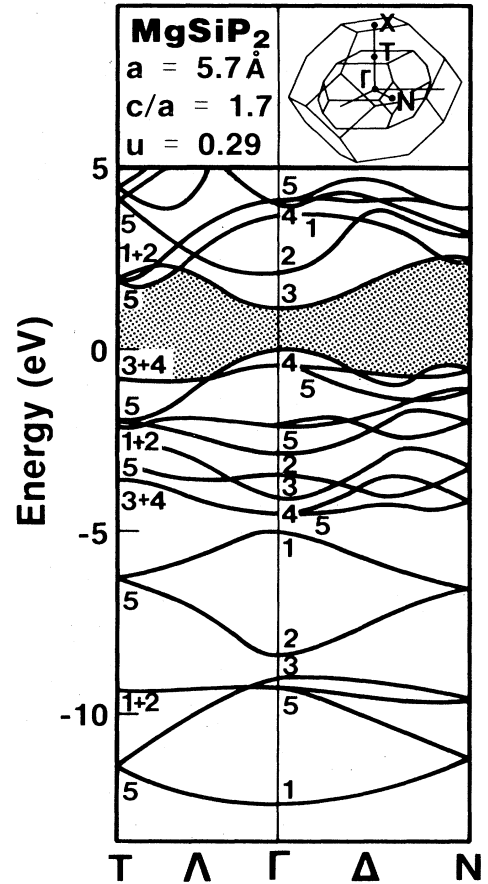


FIG. 2. Calculated band structure of  $\text{MgSiP}_2$ .

are derived from a  $\Gamma_{15v}$  state of the zinc-blende structure. The bottom of the conduction band has  $\Gamma_{3c}$  symmetry and is derived from an  $X_{3c}$  zinc-blende state. The gap is therefore pseudodirect, as indicated by experiment.<sup>18</sup> The calculated band gap is 1.0 eV, roughly half the values quoted in the literature, 2.2–2.5 eV [Ref. 19(a)], 2.24 eV [Ref. 19(b)], 2.26 eV (Ref. 18), and 2.3 eV (Ref. 17). This underestimation of the band gap is a universal feature of local-density calculations in semiconductors.<sup>20</sup>

BINARY TO TERNARY TRANSITION:  
A CONCEPTUAL FRAMEWORK

It is illuminating to compare  $\text{MgSiP}_2$  with its binary analog AIP by considering a two-step process.<sup>4(a)</sup> First, we replace the two Al atoms in a doubled zinc-blende unit cell  $\text{AlAlP}_2$  by Mg and Si without changing the geometrical structure, i.e., keeping the parameters  $a$ ,  $\eta$ , and  $u$  equal to their values in AIP:  $a_{\text{AIP}}$ ,  $\eta = 1$ , and  $u = \frac{1}{4}$ . This is used to extract the “cation electronegativity” (CE) contribution  $\Delta F^{\text{CE}}$  to the property  $F$ , reflecting the presence of two different cations which can exchange charge:

$$\Delta F^{\text{CE}} = F(\text{MgSiP}_2, a_{\text{AIP}}, \eta = 1, u = \frac{1}{4}) - F(\text{AIP}, a_{\text{AIP}}, \eta = 1, u = \frac{1}{4}). \quad (1)$$

In the second step, we allow  $(a, \eta, u)$  to relax to achieve a minimum in the total energy and study the function

$F(a, \eta, u)$ . The change in  $F$  due to the structural (S) relaxation is given by

$$\Delta F^S = F(\text{MgSiP}_2, a_{\text{eq}}, \eta_{\text{eq}}, u_{\text{eq}}) - F(\text{MgSiP}_2, a_{\text{AIP}}, \eta = 1, u = \frac{1}{4}) . \quad (2)$$

We can further decompose  $\Delta F^S$  into individual contributions due to the change in each separate structural parameter,  $\Delta F^a$ ,  $\Delta F^\eta$ , and  $\Delta F^u$ . The sum  $\Delta F^{\text{CE}} + \Delta F^S$  represents the net change in property  $F$  in going from the binary to the ternary system, each at its respective equilibrium structure.

### CATION ELECTRONEGATIVITY EFFECTS

We find that the first step of replacing the Al atoms in AIP by Mg and Si in a frozen zinc-blende lattice [Eq. (1)] is accompanied by a large transfer of charge density  $\Delta\rho^{\text{CE}}$  from the Mg to the Si sites (Fig. 3), as the Mg–P bond becomes more ionic and the Si–P bond becomes more covalent. The sensitivity of the band-structure eigenvalues to the cation replacement  $\Delta\epsilon_{nk}^{\text{CE}}$  depends on the corresponding wave functions. Large shifts of eigenvalues are found only if the corresponding wave function  $\psi_{nk}$  has a large cationic character. Such shifts contribute to optical bowing in alloys.<sup>21</sup> The threefold degenerate  $\Gamma_{15v}$  state at the top of the valence band in AIP (an *anionic p* state) is split into  $\Gamma_{4v} + \Gamma_{5v}$  by less than 0.03 eV by the CE effect, whereas the lowest  $\Gamma_{15c}$  conduction-band state (mainly a *cationic p* state), is split by

as much as 0.8 eV. The  $X_{3c}$  state at the bottom of the conduction band of AIP has most of its amplitude in the interstitial region<sup>9</sup> and therefore is only slightly affected by the cationic replacement. This insensitivity, combined with the insensitivity of the  $\Gamma_{15v}$  state, is responsible for the small dependence of the band gap on the cation electronegativity difference,  $\Delta E_g^{\text{CE}} = -0.03$  eV. Since the valence band is mainly anionic in character, most of the band structure of the unrelaxed MgSiP<sub>2</sub> is similar to the band structure of AIP folded into the chalcopyrite Brillouin zone. There are, however, a few noticeable exceptions, associated with the AIP wave functions which have large cationic character (those contributing to the partial covalent bonding character of AIP). The second lowest valence bands at  $X$  and  $W$  in AIP are such examples. They interact strongly in unrelaxed MgSiP<sub>2</sub> (having similar energies in AIP, and the same  $\Gamma_2$  symmetry in the chalcopyrite space group), and shift by 1.5–2.5 eV, giving rise to, among other features, the band associated with the Si–P bond. All of these effects are missed by virtual-crystal approaches, or by band-structure folding approaches.

### STRUCTURAL RELAXATION EFFECTS

Allowing MgSiP<sub>2</sub> to relax to its equilibrium structure [Eq. (2)] induces large changes in the internal structural parameters. Although the volume of the unit cell changes by only 0.6%, the value of  $\eta$  and  $u$  change, respectively, by 14% and 15%. The relaxation is accompanied by a lowering (i.e., stabilization) of the total energy of  $\Delta E_{\text{tot}}^S = -1$  eV per unit cell. The shifts  $\Delta\epsilon_{nk}^S$  in the band-structure energies are of order 0.5 eV. Their most noticeable effect is to lift the quasidegeneracies of the unrelaxed MgSiP<sub>2</sub> band structure. For instance, the  $\Gamma_{4v}$  and  $\Gamma_{5v}$  states at the top of the valence band, split by only 0.03 eV before relaxation, are now split by  $\Delta_{\text{CF}} = 0.5$  eV in the equilibrium geometry. The relaxation reduces the band gap by  $\Delta E_g^S = -0.49$  eV, giving a total reduction of the band gap with respect to AIP of  $\Delta E_g = \Delta E_g^S + \Delta E_g^{\text{CE}} = -0.52$  eV. This reduction of the band gap with respect to the binary analog (the “band-gap anomaly”<sup>2</sup>) is a universal feature of ternary compounds<sup>2</sup> and shares the same underlying physical mechanisms with optical bowing in semiconductor alloys,<sup>2,21</sup> i.e., the existence of two different bond lengths in the compound. This effect too is missed by virtual-crystal approaches. Notice that we observe both a *stabilization* of the total energy ( $\Delta E_{\text{tot}}^S < 0$ ) and a *reduction* of the band gap ( $\Delta E_g^S < 0$ ), in contrast with the dielectric model,<sup>22</sup> where the reduction in band gap is associated with raising the valence band, hence, a *destabilization* of the total energy. The crystal-field splitting  $\Delta_{\text{CF}}$  is rather insensitive to changes in volume at constant  $c/a$ . Increasing  $u$  slightly stabilizes  $\Gamma_{4v}$  with respect to  $\Gamma_{5v}$ , but the splitting between these two levels is more sensitive to the value of  $c/a$ . For  $\eta < 1$  the  $\Gamma_{4v}$  level (an anionic  $p_z$  state) is stabilized by the tetragonal distortion, whereas for  $\eta > 1$  the  $\Gamma_{5v}$  level (an anionic  $p_{x,y}$  state) is stabilized. This behavior shows the dominance of the next-nearest-neighbor antibonding character of the  $\Gamma_{4v}$  and  $\Gamma_{5v}$  wave functions. For ternary chalcopyrites with  $\eta < 1$  (including MgSiP<sub>2</sub>), the top of the valence band has been identified as a  $\Gamma_{4v}$  state, whereas for ternaries with  $\eta > 1$  the top of the valence band has been attributed the  $\Gamma_{5v}$  symmetry.<sup>23</sup> The sensitivity of  $\Delta_{\text{CF}}$  to the value of  $\eta$  explains the success of an empirical

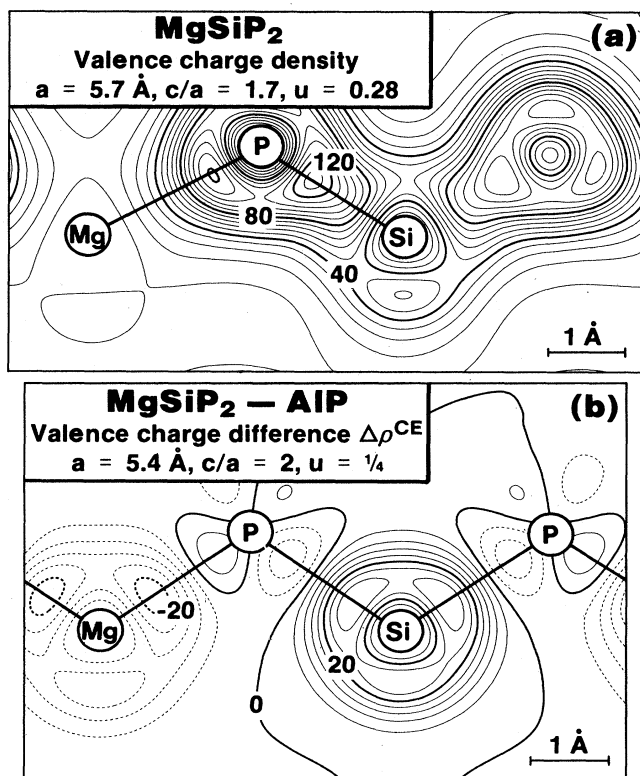


FIG. 3. (a) Valence charge density of MgSiP<sub>2</sub> at the equilibrium geometry and (b) difference  $\Delta\rho^{\text{CE}}(\mathbf{r})$  in electronic charge density between AlAIP<sub>2</sub> and unrelaxed MgSiP<sub>2</sub>. Density units are in  $e/\text{cell}$ . Different figure sizes reflect the different unit-cell size.

model<sup>24</sup> which assumes that  $\Delta_{CF}$  is proportional to  $(\eta - 1)$ .

The  $\Gamma_{3c}$  state at the bottom of the conduction band of  $\text{MgSiP}_2$  is antibonding between the phosphorus  $s$  and the cation  $p_z$  functions. It is mostly localized in the cationic interstitial site. It has antibonding character along the atomic chains in the (110) plane but is bonding along the chains in the (011) and (101) planes; it is thus stabilized by a tetragonal distortion which lowers the value of  $\eta$ .

The lifting of the degeneracy of the valence-band maximum and the stabilization of the conduction-band minimum with decreasing  $\eta$  dominate the reduction of the band gap. If in our relaxation process we first relax  $u$  and then  $\eta$  (the change in volume is so small that it gives a negligible contribution), we find  $\Delta E_g^u = 0.19$  eV and  $\Delta E_g^\eta = -0.68$  eV. If we relax in the opposite order, we find  $\Delta E_g^\eta = -0.84$  eV and  $\Delta E_g^u = 0.35$  eV. In both cases, the total structural contribution  $\Delta E_g^S = \Delta E_g^u + \Delta E_g^\eta = -0.49$  eV reduces the band gap because the tetragonal distortion lowers the band gap more than the anionic displacement increases it.

The sensitivity of the band gap to tetragonal distortions is reflected in the deformation potentials, i.e., the energy derivatives of the band gap with respect to the structural parameters. At the equilibrium geometry we find

$$a \frac{\partial E_g}{\partial a} = 0.5 \text{ eV}, \quad c \frac{\partial E_g}{\partial c} = 5.8 \text{ eV}, \quad u \frac{\partial E_g}{\partial u} = 2.4 \text{ eV} \quad (3)$$

Previous results<sup>2(b)</sup> on other II-IV-V<sub>2</sub> pnictides have similarly yielded a  $W_1$ -phonon deformation potential of  $u(\partial E_g/\partial u) \approx 3$  eV. We have found also that, whereas the dependence of  $E_g$  on  $a$  and  $u$  is mostly linear, the dependence on  $c$  has a strong nonlinear contribution. This decomposition shows that the anomalously small band gap of  $\text{MgSiP}_2$  can be understood in terms of the response of the band struc-

ture to *internal strain* exerted by variations in  $\eta$  and  $u$  (with smaller contributions due to volume change and the CE effect). It was previously pointed out<sup>2,4(a),21</sup> that the same mechanism is responsible for optical bowing in alloys and I-III-VI<sub>2</sub> chalcopyrites.

## CONCLUSIONS

The first *ab initio* geometry optimization of a ternary semiconductor reproduces correctly its structural parameters and has been used to predict a phonon frequency and a few elastic constants. Using this system as a model for the physical changes attendant upon transition from a binary to a ternary system, we find such modifications to be usefully classified as "chemical" (CE) and "structural" (S). The chemical change is characterized by a charge redistribution  $\Delta\rho^{\text{CE}}(\mathbf{r})$  and nonrigid band-dependent shifts  $\Delta\epsilon_{nk}^{\text{CE}}$  in eigenvalues, distinguishing band states which have amplitude on the modified sublattice (which shift) from those confined to the common sublattice (which do not). The structural change is highlighted by the fact that although the volume-per-atom ratio is nearly conserved by relaxation, internal structural degrees of freedom ( $u, \eta$ ) change by as much as 15%. This is accompanied by a large stabilization of the total energy and a substantial band-gap narrowing, usefully characterized as the response of the band structure to *internal stress*, imposed by the alternating bond lengths (a  $W_1$  frozen phonon mode) and tetragonal deformations.

## ACKNOWLEDGMENT

This work was supported in part by the Office of Energy Research, Materials Science Division, U.S. Department of Energy, Grant No. DE-AC02-77-CHO-0178.

<sup>1</sup>E. Parthé, *Crystal Chemistry of Tetrahedral Structures* (Gordon and Breach, New York, 1964).

<sup>2</sup>(a) J. E. Jaffe and A. Zunger, *Phys. Rev. B* **29**, 1882 (1984); (b) **30**, 741 (1984).

<sup>3</sup>J. C. Mikkelsen and J. B. Boyce, *Phys. Rev. Lett.* **49**, 1412 (1982).

<sup>4</sup>(a) G. P. Srivastava, A. Zunger, and J. L. Martins, *Phys. Rev. B* **31**, 2561 (1985); (b) T. S. Kuan, T. F. Kuech, W. I. Wang, and E. L. Wilkie, *Phys. Rev. Lett.* **54**, 201 (1985).

<sup>5</sup>See reviews in *GaInAsP Alloy Semiconductors*, edited by T. P. Pearsall (Wiley, New York, 1982).

<sup>6</sup>J. Ihm, A. Zunger, and M. L. Cohen, *J. Phys. C* **12**, 4409 (1979).

<sup>7</sup>J. P. Perdew and A. Zunger, *Phys. Rev. B* **23**, 5048 (1981).

<sup>8</sup>G. B. Bachelet, D. R. Hamann, and M. Schlüter, *Phys. Rev. B* **26**, 4199 (1982).

<sup>9</sup>D. Wood and A. Zunger, *J. Phys. A* **18**, 1343 (1985).

<sup>10</sup>P. Bendt and A. Zunger, *Phys. Rev. B* **26**, 3114 (1982).

<sup>11</sup>A. A. Vaipolin, *Fiz. Tverd. Tela* **15**, 1430 (1973) [*Sov. Phys. Solid State* **15**, 965 (1973)].

<sup>12</sup>S. Froyen and M. L. Cohen, *Phys. Rev. B* **28**, 3258 (1983).

<sup>13</sup>L. D. Landau and E. M. Lifshitz, *Theory of Elasticity* (Pergamon, Oxford, 1970).

<sup>14</sup>H. J. McSkimin and P. Andreatch, Jr., *J. Appl. Phys.* **35**, 2161 (1964).

<sup>15</sup>I. P. Kaminow, E. Buehler, and J. H. Wernick, *Phys. Rev. B* **2**, 960 (1970); see compilation in A. Miller, A. MacKinnon, and D. Weaire, in *Solid State Physics*, edited by H. Ehrenreich, F. Seitz, and D. Turnbull (Academic, New York, 1981), Vol. 36.

<sup>16</sup>A. S. Poplavnoi, Y. I. Polygalov, and V. A. Chaldyshev, *Izv. Vyssh. Uch. Zav. Fiz.* **6**, 95 (1970) [*Sov. Phys. J.* **13**, 766 (1970)]; N. A. Goryunova, A. S. Poplavnoi, Y. I. Polygalov, and V. A.

Chaldyshev, *Phys. Status Solidi* **39**, 9 (1970); A. S. Poplavnoi, Y. I. Polygalov, and A. M. Ratner, *Fiz. Tekh. Poluprovodn.* **16**, 702 (1982) [*Sov. Phys. Semicond.* **16**, 451 (1982)].

<sup>17</sup>A. N. Gusatinskii, M. A. Bunin, M. A. Blokhin, V. I. Minin, V. D. Prochukhan, and G. K. Averkieva, *Phys. Status Solidi* (b) **100**, 739 (1980).

<sup>18</sup>G. K. Averkieva, A. Mamedov, V. D. Prochukhan, and Y. V. Rud', *Fiz. Tekh. Poluprovodn.* **12**, 1732 (1978) [*Sov. Phys. Semicond.* **12**, 1025 (1978)].

<sup>19</sup>(a) R. Trykozko and N. A. Goryunova, *Izv. Akad. Nauk SSSR, Ser. Neorg. Mater.* **4**, 2101 (1968) [*Inorg. Mater.* **4**, 1826 (1968)]; (b) A. J. Spring Thorpe and J. G. Harrison, *Nature* **222**, 977 (1969).

<sup>20</sup>See compilation in A. Zunger, *J. Vac. Sci. Technol.* **16**, 1337 (1979), and an early discussion of the problem in A. Zunger and A. J. Freeman, *Phys. Rev. B* **16**, 2901 (1977).

<sup>21</sup>A. Zunger and J. E. Jaffe, *Phys. Rev. Lett.* **51**, 662 (1983).

<sup>22</sup>J. A. Van Vechten, in *Semiconductor Handbook*, edited by S. P. Keller (North-Holland, Amsterdam, 1980), Vol. 3, p. 1.

<sup>23</sup>G. K. Averkieva, G. A. Medvedkin, and A. A. Yakovenko, *Fiz. Tekh. Poluprovodn.* **17**, 2081 (1983) [*Sov. Phys. Semicond.* **17**, 1330 (1983)].

<sup>24</sup>J. L. Shay and J. H. Wernick, *Ternary Chalcopyrite Semiconductors: Growth, Electronic Properties and Applications* (Pergamon, Oxford, 1975).

<sup>25</sup>C. C. Wang, M. Zaheeruddin, and L. H. Spinar, *J. Inorg. Nucl. Chem.* **25**, 326 (1961).

<sup>26</sup>K. Godwod, R. Kowakyzk, and Z. Szmid, *Phys. Status Solidi* (a) **21**, 227 (1974).